# *Ab initio* calculation of the metal-insulator transition in lithium rings

Beate Paulus, Krzysztof Rosciszewski,* and Peter Fulde

*Max-Planck-Institut für Physik komplexer Systeme, Nöthnitzer Straße 38, D-01187 Dresden, Germany*

Hermann Stoll

*Institut für Theoretische Chemie, Universität Stuttgart, D-70550 Stuttgart, Germany*

We study how the Mott metal-insulator transition (MIT) is affected when we have to deal with electrons with different angular momentum quantum numbers. For that purpose we apply *ab initio* quantum-chemical methods to lithium rings in order to investigate the analog of a MIT. By changing the interatomic distance we analyze the character of the many-body wave function and discuss the importance of the $s$-$p$ orbital quasidegeneracy within the metallic regime. The charge gap (ionization potential minus electron affinity) shows a minimum, and the static electric dipole polarizability has a pronounced maximum at a lattice constant where the character of the wave function changes from significant $p$ to essentially $s$ type. In addition, we examine rings with bond alternation in order to answer the question that under which conditions a Peierls distortion occurs.

## I. INTRODUCTION

When the lattice constant of a metallic system is sufficiently enlarged it will become an insulator, before eventually we end up with a collection of well separated atoms. This metal to insulator (MI) transition was first pointed out by Mott (Ref. 1, and references therein) and has stimulated a tremendous amount of work for a better understanding of it. The standard model for these investigations has been the Hubbard Hamiltonian.[2] It assumes one orbital per site, and the electronic Coulomb interactions are reduced to an on-site Coulomb integral $U$. By applying different approximations Hubbard was able to quantify the conditions for the occurrence of a MI phase transition. For that reason it is often called a Mott-Hubbard transition. More recently, the dynamical mean-field theory has been applied to the Hubbard Hamiltonian with one electron per site and has further elucidated details of the transition (for an overview and further references see, e.g., Ref. 3).

The purpose of the present work is to go beyond the Hubbard model in order to understand better how other features might influence the transition in a realistic system. Lithium is a metal with a strong contribution of $p$ electrons to the conduction band. With increasing lattice constant the ratio of $p$ and $s$ electrons is changing and in the atomic limit we are dealing with a pure $1s^2 2s$ atomic state. One of the questions we would like to answer is the effect of low-energy atomic excitations from $2s$ to $2p$ on the MI transition. In order to come close to a realistic description of metallic systems we investigate a ring of Li atoms applying quantum-chemical methods for a treatment of electronic correlations.

In terms of a Hubbard model the Li-Li distance would correspond to the hopping term $t$. Instead of only an on-site Coulomb repulsion as in the Hubbard model here we take into account all possible Coulomb matrix elements. But in the limit of large separations of atoms only the on-site Coulomb repulsion remains.

The largest ring which we can treat at the multireference configuration-interaction (MRCI) level, without excessive computations, consists of ten Li atoms. A medium-size basis set consisting of Gaussian-type orbitals (GTO's) is used in the calculations. Usually the onset of insulating behavior is characterized by the appearance of a gap. However, with a finite number of Li atoms in the ring we always have a finite-energy difference between consecutive energy levels. Therefore, when the atomic distance is changed we must look for a change in the pattern between the highest occupied molecular orbital (HOMO) and the lowest unoccupied orbital (LUMO). These quantities are only accessible at the mean-field level. At the correlated level, we select three quantities which can give insight as regards the transition behavior. MRCI methods can yield very good approximations to the exact ground-state wave function. The character of this wave function will be the first criterion. A second quantity which we calculate is the one-particle energy gap defined as the energy difference which is obtained if an electron is added to or removed from the system. As a third quantity, we determine the static dipole polarizability of the system by applying a small homogeneous electric field. These three quantities are determined as functions of the nearest-neighbor Li-Li distance in the ring, and we discuss how the metal-insulator transition shows up in them. For these quasi-one-dimensional systems, the question arises whether we can gain energy by dimerization (Peierls distortion). We address this question by allowing for a bond alternation.

In the following section we will discuss some technical details (Sec. II). In Sec. III, we present the results of different mean-field methods, for Li rings with increasing number of Li atoms and with increasing Li-Li distance. The behavior of the many-body wave function is discussed in Sec. IV. Gap energies are presented in Sec. V and polarizabilities in Sec. VI. The Peierls distortion is considered in Sec. VII and conclusions follow in Sec. VIII.

## II. TECHNICAL DETAILS

The application of quantum-chemical *ab initio* methods to Li rings is the focus of the present work. Starting from a

TABLE I. ACPF values of the ionization potential (IP), the electron affinity (EA), and the dipole polarizaibility $\alpha$ of the Li atom are listed for different basis sets. Corresponding values for the bond length $d_{dimer}$ of the Li$_2$ molecule are listed, too.

| Basis set | IP (a.u.) | EA (a.u.) | $\alpha$ (a.u.) | $d_{dimer}$ (Å) |
|---|---|---|---|---|
| aug-cc-pVDZ | 0.196 | 0.0151 | 166.0 | 2.73 |
| aug-cc-pVTZ | 0.196 | 0.0176 | 167.2 | 2.69 |
| aug-cc-pVQZ | 0.196 | 0.0209 | 167.5 | 2.68 |
| $[4s]$ | 0.196 | 0.0019 | 0.000 | 3.03 |
| $[3s1p]$ | 0.196 | 0.0150 | 164.8 | 2.85 |
| $[4s1p]$ | 0.196 | 0.0212 | 165.6 | 2.85 |
| $[4s2p]$ | 0.196 | 0.0216 | 165.6 | 2.73 |
| $[5s2p]$ | 0.196 | 0.0218 | 166.6 | 2.67 |
| Expt. | 0.198 (Ref. 11) | 0.0227 (Ref. 11) | 164.8 (Ref. 13) | 2.67 (Ref. 11) |

mean-field Hartree-Fock (HF) description, we reoptimize the valence wave function in multiconfiguration self-consistent-field (MCSCF) calculations, keeping the 1$s$ core electrons frozen at the HF level. Thereby, the number of valence active-space orbitals is chosen equal to (or larger than) the number of Li atoms of the system, and all possible occupations of these orbitals are accounted for. With this choice, we can properly describe the dissociation limit where each atom has one valence electron. On top of the MCSCF calculations, we apply the multireference averaged coupled pair functional (MRACPF) method.[4,5] Here, all configuration-state functions are included which can be generated from the MCSCF reference wave function by means of single and double excitations from the active orbitals. These calculations are performed with the program package MOLPRO.[6–8]

The GTO one-particle basis set used for the MCSCF/MRACPF calculations of the present work is derived from the correlation-consistent polarized valence double-$\zeta$ (cc-pVDZ) basis set of Dunning and co-workers.[9] From this set, we select the three $s$ functions and the first contracted $p$ function. To describe the negatively charged system, we add an even-tempered diffuse $s$ function (exponential parameter is 0.0107) resulting in a $[4s1p]$ basis set. We checked the quality of this basis by calculating the electron affinity (EA), the ionization potential (IP), and the dipole polarizability of the Li atom (Table I). The $p$ function is essential to describe the EA and the polarizability properly. Whereas the IP is weakly dependent on the size of the basis set used, because correlation effects are absent (core-valence correlation is neglected), the EA substantially increases when a diffuse $s$ function is added. A second diffuse $s$ function or a diffuse $p$ function has nearly no influence. The polarizability only slightly depends on the basis-set quality beyond cc-pVDZ, if the basis set contains at least one $p$ function. The errors of the selected $[4s1p]$ basis set as compared with experimental data are 1% for the IP, 7% for the EA, and 0.5% for the polarizability. Thus, the $[4s1p]$ basis although being relatively small can describe with sufficient accuracy all quantities we are interested in and is taken as default basis set in the subsequent calculations.

The Li-Li distance in three-dimensional Li metal is $a_0 = 3.03$ Å,[10] while the equilibrium distance of the Li$_2$ dimer (2.67 Å, Ref. 11) is smaller by about 10%. For the Li$_{10}$ ring,

we calculate an equilibrium distance of 3.06 Å, which is very similar to the bulk nearest-neighbor distance. Note, however, that the $[4s1p]$ basis overestimates the Li$_2$ bond length by 0.18 Å (the lack of a second $p$ function is mainly responsible for this error, cf. Table I); if this bond-length error carries over to Li$_{10}$, we would have an equilibrium distance of around 2.9 Å for this system.

## III. MEAN-FIELD DESCRIPTION

As a first step of our MIT study for Li rings, we performed mean-field [Hartree-Fock and density-functional (DFT)] calculations for various ring lengths and internuclear distances. With the CRYSTAL program[12] we can do HF calculations for the one-dimensional infinite Li chain. As basis set we selected the optimized $[3s2p]$ basis set for the three-dimensional metal.[14] In Fig. 1, the HF band structure is shown for the bulk equilibrium internuclear distance $a_0$, and for $a = 2.5a_0$ which corresponds to the dissociation limit. In both cases the Fermi energy lies within the 2$s$ band, but the
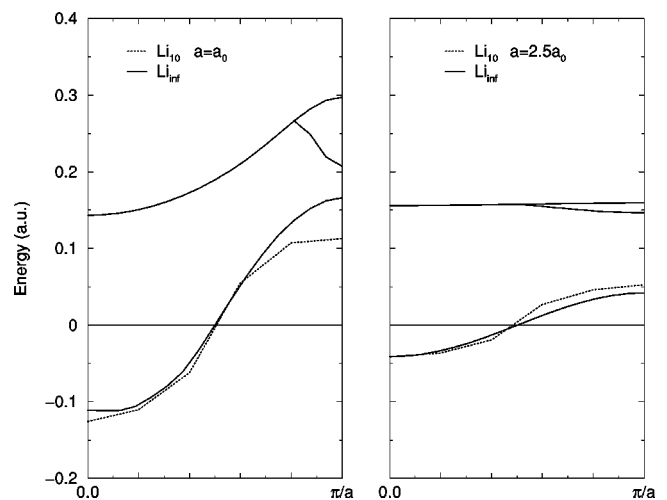


FIG. 1. Hartree-Fock band structure for the infinite Li chain for two different Li-Li distances. The Fermi energy is set to zero. In addition, a band structure obtained from the levels of Li$_{10}$ is plotted (dashed curve); for comparison, the center of the 2$s$ band is shifted to zero.
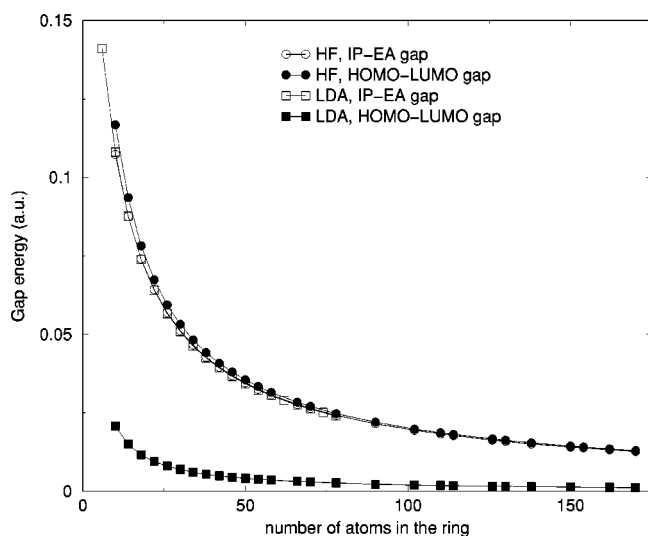
FIG. 2. Mean-field results (HF and LDA) for finite Li rings, in dependence of the number of atoms in the ring. The Li-Li distance is fixed at the metallic value ($a = a_0$).



FIG. 3. Mean-field results [HF in $D_{10h}$ symmetry, DFT (LDA and GGA) in $D_{2h}$ symmetry] for a $Li_{10}$ ring, in dependence of the Li-Li distance. The gap energy is taken as the difference of IP and EA; in the HF case, also the HOMO-LUMO gap value is given.

bandwidth is significantly reduced with increasing Li-Li distance. The predominant $2p$ band is very flat near the dissociation limit and well separated from the $2s$ band, whereas for a distance $a_0$ there is no gap between the $2s$ and $2p$ bands.

For finite systems we applied the TURBOMOLE *ab initio* program package[15] to obtain mean-field results for very long rings up to $n = 170$. We explicitly imposed spatial-symmetry restrictions on our closed-shell wave functions in order to avoid symmetry breaking. (For rings with $n > 30$, the HF approximation favors a symmetry-broken ground state.) If we generate a HF band structure from the orbital energies of a $Li_{10}$ ring and shift the Fermi energy to zero (dashed curve in Fig. 1), the bandwidth and band shape correspond well to that of the infinite chain, for both $a = a_0$ and $a = 2.5a_0$.

The energy gap of Li rings with different number of atoms, at a fixed Li-Li distance of $a = a_0$, is shown in Fig. 2. In a mean-field approach, the gap energy can either be calculated as HOMO-LUMO gap in the neutral system or by adding and subtracting an electron to the system, i.e., as difference of the IP and EA. At the HF level both approaches (approximately) coincide according to Koopmans' theorem.[16] Slight differences occur for smaller rings due to relaxation of the orbitals when the electron number is changed. This effect is missing in the HOMO-LUMO gap. Calculating the IP-EA gap with density-functional theory in the local-density approximation (LDA),[17] the results coincide well with the HF results. Note that in LDA the HOMO-LUMO gap is much smaller. This gap is directly related to an excitation energy other than the IP-EA gap. The decay of the IP-EA gap with increasing number of atoms in the ring is slow ($n^{-0.76}$). [If we would regard the finite ring as consisting of free electrons in a box, the decay should be proportional to $(boxlength)^{-1}$.] Despite the slow closing of the gap, even for $Li_{10}$ it lies well within the bandwidth of the infinite chain. For the $Li_{10}$ ring, we also calculated the behavior of the IP-EA gap with increasing Li-Li distance, from
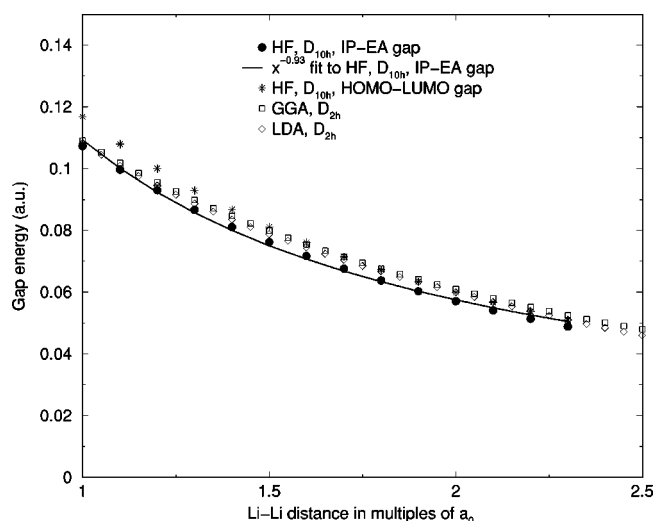
$a_0$ to $2.5a_0$ (Fig. 3). For the mean-field approaches, HF and DFT [both LDA, Ref. 17 and generalized gradient approximation, GGA, Refs. 18 and 19], the gap is monotonously closing. Thereby, the differences between the DFT variants and the differences between DFT and HF are not larger than that between the HOMO-LUMO and IP-EA values at the HF level. [Small differences may also arise due to the use of different formal symmetries ($D_{2h}$ for DFT, $D_{10h}$ for HF).] If we would model the ring by free electrons in a box again, the decay of the HOMO-LUMO gap should be proportional to $(boxlength)^{-2}$. This is in contrast to an approximate $a^{-1}$ decrease obtained in our mean-field calculations, which shows that the electrons are far away from the free-electron limit. It should be kept in mind, however, that the correct dissociation limit cannot be described with these methods, anyway. Only multiconfiguration methods can properly describe both the dissociation limit and the metallic behavior.[22] Such calculations form the main part of our present work and will be discussed below.

## IV. THE CHARACTERISTIC FEATURES OF THE GROUND-STATE WAVE FUNCTION

Taking the example of the $Li_{10}$ ring, we want to study how the character of the many-body ground-state wave function changes when enlarging the Li-Li distance from $a = a_0$ to $a = 2.5a_0$. For that purpose we performed a MCSCF calculation[20,21] for the lowest singlet state, on top of a closed-shell HF calculation such as that described in the preceding section. (Using the MOLPRO package, we had to formally change to $D_{2h}$ symmetry, however.) The selection of the active space is a decisive step: It is well known that for a correct description of the dissociation limit in $Li_{10}$ ten atomic $2s$ orbitals are needed, but for the metallic regime ($a \approx a_0$) it is not clear how many orbitals are really important. Therefore, we performed a pilot MCSCF calculation for $a = a_0$ with a high number of active orbitals and selected those
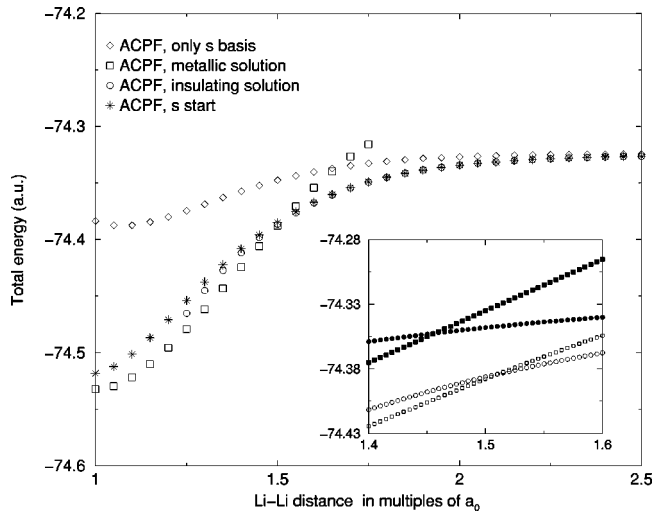
FIG. 4. MRACPF energies of the $Li_{10}$ ring vs the Li-Li distance. The curves labeled "insulating wave function" and "metallic wave function" refer to different MCSCF zeroth-order wavefunctions used as reference for the subsequent MRACPF, cf. text. In the inset an enlarged part of the transition region is shown. The filled symbols correspond to the MCSCF values. The curves labeled "$s$ start" and "only $s$ basis" refer to calculations leaving out $p$ functions in the MCSCF zeroth-order wave functions and at both the MCSCF and MPACPF levels, respectively.

natural orbitals whose occupancies were above a certain threshold. Retaining orbitals with occupancies larger than 0.18 and rejecting all the others which have occupancies smaller than 0.03 resulted in ten active orbitals, too. However, only the nine energetically lowest ones fall into the same irreducible representations (in $D_{2h}$ symmetry) as the nine lowest-lying orbitals of the insulating regime, while the highest natural orbital of the metallic and insulating regime differs in symmetry. Therefore, we selected for our final MCSCF calculation a new set of 11 active orbitals which was generated as the union of the two sets of orbitals described above. These orbitals were reoptimized at the MCSCF level. Finally, we performed a MRACPF calculation[4,5] on top of the MCSCF, in order to include dynamical correlation effects as fully as possible. Note that the multireference treatment is important in both limits: in the metallic regime to describe static correlation with the quasidegenerate $2p$ orbitals and in the insulating regime to get the dissociation into degenerate $2s$ orbitals right.

Although we included in the active space all orbitals which are important in the limits of small and large atomic distances, the total energy as a function of the Li-Li distance is not a smooth curve (Fig. 4). This is so because the nature of the active orbitals changes along the curve. When starting the calculations from large $a$ (wave function for the insulating state) and always using the previous solution as starting point for the next smaller lattice constant, this yields a slightly different solution in the region of the MIT than when starting from the metallic regime and increasing $a$. The difference is larger, of course, for the MCSCF energies than at the MRACPF level, with a full CI (i.e., including all higher excitations) the differences would vanish. However, a single
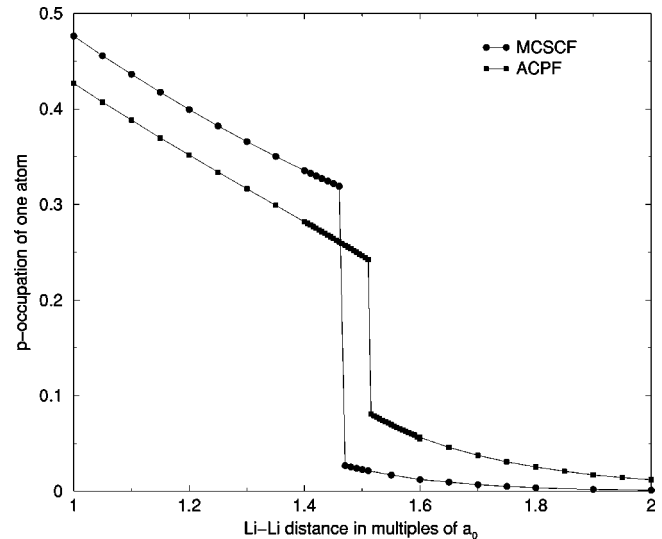


FIG. 5. The $p$ occupation of the Li atom in a $Li_{10}$ ring vs the Li-Li distance. The $p$ occupations are calculated with the Mulliken population analysis.

smooth curve can be obtained even at the MRACPF level if it is based on a MCSCF calculation with only $s$ functions in the active space. In that case $p$ excitations appear at the MRACPF level only. It is clear that such a procedure favors the insulating solution: It yields a ground-state energy for $a = a_0$ which is by $\sim 0.02$ a.u. higher than the value obtained with variationally optimized MCSCF orbitals. Still, the so obtained ground-state potential curve is qualitatively correct also in the metallic regime. It is interesting to compare it with a MRACPF curve obtained by leaving out $p$ functions in the one-particle basis set altogether. Here, we still observe a (shallow) minimum near $a = a_0$, but the energy is higher by more than 0.1 a.u. Thus, $p$ contributions amount to about two-thirds of the binding energy of the $Li_{10}$ ring.

Turning back now to our most accurate potential curve the change of the character of the MRACPF wave function as well as that of the underlying MCSCF wave function as a function of $a$ is seen best by a Mulliken population analysis for the $p$ orbitals (Fig. 5). For the "metallic" MCSCF solution the atomic $p$ orbital occupancy is nearly 0.5 at $a = a_0$ and slowly drops to 0.3 at $a \approx 1.5a_0$, while for the "insulating" solution it is less than 0.03 for $a \geq 1.5a_0$. Even in the MRACPF case, the $p$ population changes by a factor of $\sim 3$. Taking this rather dramatic change as a signature of the MIT we find for all investigated rings a region around $1.5a_0$, where the character of the wave function changes significantly.

## V. THE ONE-PARTICLE ENERGY GAP

The energy gap of an insulator is determined by the energy differences between the ground state of the neutral system and the ones with one electron added and subtracted. In the case of a Li ring, we calculate the MRACPF ground-state energies of the $Li_n^-$, $Li_n$, and $Li_n^+$ systems and determine $EA = E(Li_n) - E(Li_n^-)$ and $IP = E(Li_n^+) - E(Li_n)$, and from IP-EA the corresponding gap. For a metallic solid adding and
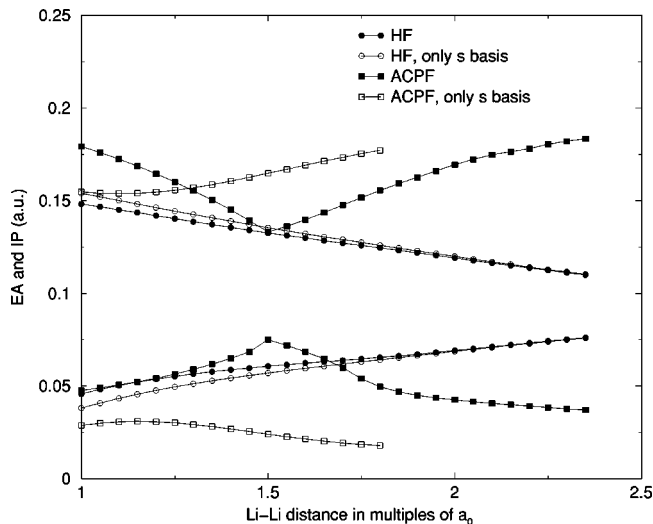
FIG. 6. HF and MRACPF values for the EA and IP of a $Li_{10}$ ring vs the Li-Li distance. For comparison, we add results from calculations without $p$ functions in the basis set ("only $s$ basis").
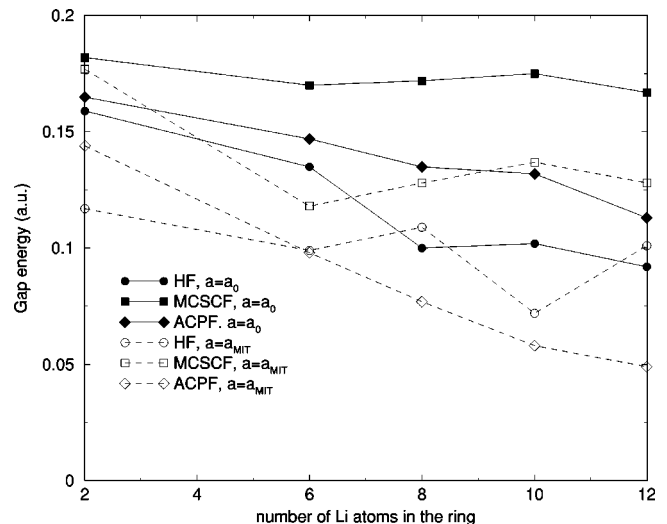


FIG. 7. HF, MCSCF, and MRACPF one-particle energy gaps are plotted vs the number of Li atoms in the ring for two different lattice constants, cf. text.

removing an electron cost an energy given by the chemical potential. In finite systems, there always remains the difference between the one-particle energies of the additional and the missing electron as well as the influence of relaxation and correlation effects.

The EA and IP for $Li_{10}$ are plotted in Fig. 6. In the metallic regime, the HOMO-LUMO gap is expected to decrease with increasing Li-Li distance exactly like it happens for free electrons in a box with changing length. In fact, at the HF level we obtain a monotonous shrinking of the gap, both with our standard basis set ($[4s1p]$) and with a pure $s$ basis set ($[4s]$). The availability of $p$ polarization functions stabilizes the charged systems as compared to the neutral one, leading to a slightly smaller gap for $a=a_0$ than with a pure $s$ basis, but the difference goes to zero for $a \to \infty$, and the general trend of a closing gap with enlarging Li-Li nearest-neighbor distance is the same in both cases. However, the trend completely changes when correlation effects are included. The most important change concerns the $a \to \infty$ limit, where HF fails to describe correctly the dissociation. Instead of a closing of the gap, the correct limit is the difference between the atomic IP and EA. This limit is obtained indeed, in our MRACPF calculations. As already noted in Sec. II, the atomic EA is severely underestimated in the case of a pure $s$ basis set, but this is efficiently remedied with our standard $[4s1p]$ basis set. We furthermore note that the EA converges more slowly to the atomic limit than IP [$EA(a=2.35a_0)$ $=1.6$ EA(atom),$IP(a=2.35a_0)=0.94$ IP(atom)]. We think that this is due to the larger size of the $Li^-$ ion than of the $Li^+$ ion. Interestingly, the variation of IP and EA from $a$ $=a_0$ to $a \to \infty$ is not completely monotonous. Already for the case of a pure $s$ basis, the gap is nearly constant (and even slightly decreases) in the range $a_0 < a < 1.3a_0$, and only then gradually opens up to the atomic limit. Including $p$ contributions leads to a significant increase of IP and EA for $a=a_0$ as well as to a distinctly nonmonotonous behavior of the gap as a function of $a$, with a minimum around $a=1.5a_0$. The effect

is due to a stabilization of the charged systems, with respect to the neutral one, by means of polarization clouds around holes/electrons. Thus, for a finite ring in the metallic regime the gap closes when enlarging the lattice constant, at the metal-insulator transition (MIT) point it is minimal, then it starts to increase gradually approaching the atomic limit value.

We investigated the gap behavior not only for the $Li_{10}$ ring but also for the $Li_2$ dimer, for the $Li_6$ and $Li_8$ rings, and for the $Li_8$ cube. ($Li_4$ arranged in a square has a negative EA; hence, the calculation of the one-particle energy gap does not make any sense. Li rings with odd number of Li atoms do not have a closed-shell HF ground state and therefore are not considered here.) For $Li_{12}$, we performed calculations at $a=a_0$ and $a=a_{MIT}^*$, where $a_{MIT}^*$ is defined as the point where the character of the MCSCF wave function changes from significant $p$ character to an essentially $s$ one. For all investigated ring systems, the minimal value of the gap occurs for nearly the same lattice constant in different rings (between $1.42a_0$ and $1.55a_0$). This distance coincides approximately with the one where the character of the wave function changes. In Fig. 7 the energy gap at $a=a_0$ and $a$ $=a_{MIT}$ is listed for different methods and for different ring lengths. When increasing the number of atoms in the ring, the minimal gap energy at the ACPF level decreases faster than the gap at $a=a_0$. Unfortunately, the behavior of the gap for much longer rings cannot be calculated by the methods we use because it is computationally too expensive. The gap calculated at the MCSCF level seems to saturate for longer rings, i.e., only the dynamical correlations are closing the gap. As yet, we cannot make a reasonable extrapolation and find out for which ring length a zero gap is to be expected. But for all investigated rings we found similar behavior with increasing Li-Li distance independent of the number of Li atoms in the ring. In spite of this we reemphasize that although we have a finite system instead of a real metallic system, we still see a transition from a metalliclike regime

TABLE II. The EA and IP of $Li_6$ are listed for different levels of approximations and different Li-Li distances.

| $a = a_0$ | EA | IP |
| --- | --- | --- |
| HF | 0.0208 | 0.1554 |
| MCSCF | −0.0027 | 0.1672 |
| ACPF | 0.0335 | 0.1812 |
| FCI | 0.0321 | 0.1820 |
| $a = 1.5 a_0$ | | |
| ACPF | 0.0539 | 0.1530 |
| FCI | 0.0500 | 0.1548 |
| $a = 2.0 a_0$ | | |
| ACPF | 0.0448 | 0.1703 |
| FCI | 0.0409 | 0.1707 |

(where the gap is closing with increasing Li-Li distance) to an insulating regime where the gap is opening towards the atomic limit.

In order to validate the methods used in the present paper, we performed full-CI (FCI) calculations[23] for $Li_6$ at three different lattice constants, i.e., we determined the lowest variational energies in each case which can be obtained with our standard $[4s1p]$ one-particle basis set. The resulting EA and IP are listed in Table II. The ACPF values coincide well with the FCI results and therefore are expected to provide a reliable, quantitative description of the gap energy.

Finally, let us note that we observe a similar minimal gap for the $Li_8$ cube, where no sharp jump in the $p$ occupation pattern of the wave function is visible. In the cube, the minimal gap occurs at a somewhat larger distance ($1.65a_0$) than it does in the ring and is also a little bit larger (0.09 a.u.), but the qualitative behavior remains the same.

## VI. DIPOLE POLARIZABILITY

As a third quantity which can be used to define the MIT, we calculate the static electric dipole polarizability of the system. We apply a static electric field of strength up to 0.035 a.u. and perform a quadratic fit for the energy of the system, $E(\mathcal{E}) = E(0) - \frac{1}{2}\alpha\mathcal{E}^2$, yielding the polarizability $\alpha$. Higher-order terms can be neglected for the small field strengths we chose. For a metallic system the polarizability should be infinite, therefore a steep increase of the polarizability can indicate an insulator-metal transition.

As a test example, we selected the $Li_2$ dimer and applied the $\mathcal{E}$ field both in the bond direction and in a direction perpendicular to that, while gradually enlarging the Li-Li distance (Fig. 8). At the equilibrium bond length, we obtain an average polarizability of 118 a.u. (the experimental value is 111 a.u., Ref. 24). If the electric field is parallel to the bond direction, the polarizability exhibits a maximum at a Li-Li distance similar to that where the minimal gap occurs. For a field direction perpendicular to the bond, the polarizability increases monotonously to two times the atomic value as the HOMO-LUMO gap becomes smaller.

For the $Li_{10}$ ring, we find the same behavior as in the dimer when we apply the field perpendicular to the ring
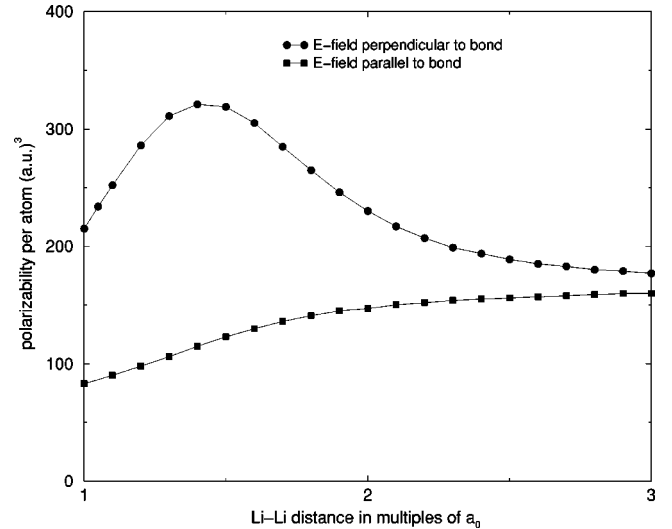


FIG. 8. The MRACPF static dipole polarizability of the $Li_2$ dimer, for the electric field parallel and perpendicular to the bond direction, is plotted vs the Li-Li distance.

plane. When we apply the field in the ring plane we find a pronounced maximum. In Fig. 9, we plot the polarizability per atom for the $Li_{10}$ ring, both at the MCSCF and MRACPF levels. A crossing of the curves occurs within the transition region, since we have two different solutions at the transition. MCSCF and MRACPF polarizability values differ only slightly. At $a = a_0$ the calculated MRACPF value is 94.4 a.u. Experimental data are available for the static dipole polarizability of a $Li_{10}$ cluster;[25] unfortunately the cluster geometry is not fully known, but it can be supposed to be two or three dimensional. The experimental value is 70.2 a.u. and it roughly agrees with our value. As already noted, the polarizability increases with decreasing lattice constant (i.e., when coming from the insulating side). For an infinite system the polarizability should diverge at the MIT. We see a precursor
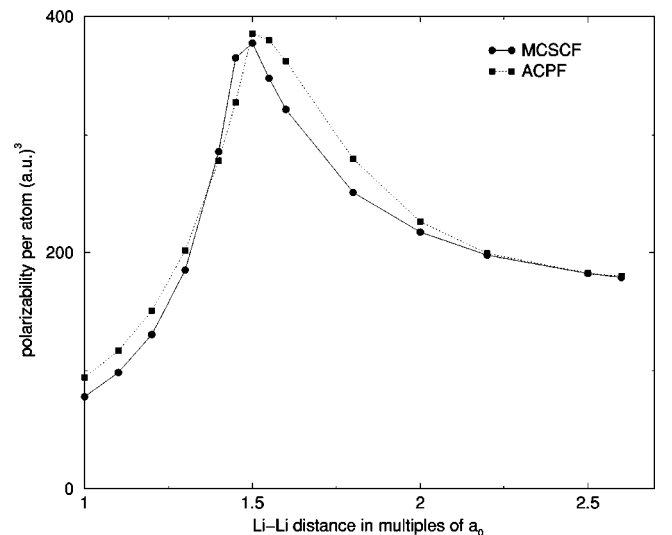


FIG. 9. The static dipole polarizability of the $Li_{10}$ ring, for the electric field in the ring plane, is plotted vs the Li-Li distance for two different methods.
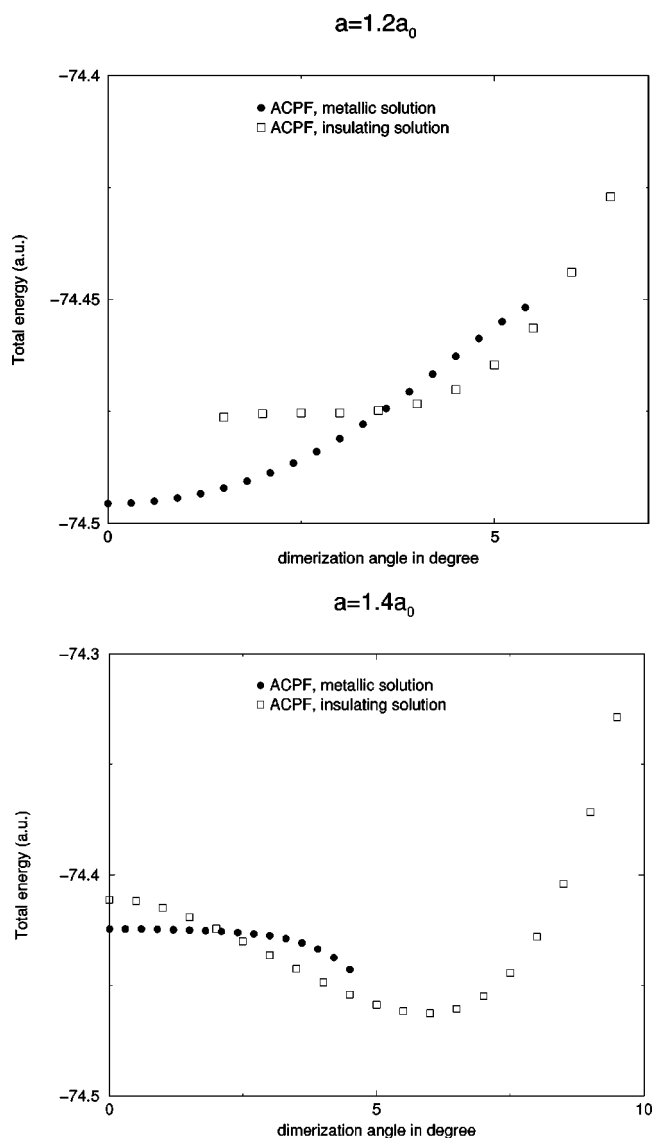
FIG. 10. The total energy of the $Li_{10}$ ring is plotted vs the dimerization angle (defined as deviation from the ideal 36° angle in $Li_{10}$, in degree) for different average lattice constants.

of this divergence and can therefore use it to define a MIT even for a finite system. The rapid decay of the polarizability in both the metallic and the insulating regime is due to the opening of the gap.

## VII. LATTICE DISTORTION

In this section, we allow for a bond alternation along the ring, so that the Li atoms can form dimers. For average lattice constants larger than that where the MI transition occurs (i.e., for lattice constants where the insulating solution is the ground state) the formation of dimers is energetically favored. The resulting dimer internuclear distance agrees well with the calculated distance of the free dimer (2.88 Å). The energy gain is due to bond formation between two Li atoms. In the metallic regime ($a \lesssim a_{MIT}$) a Peierls distortion[26] occurs, stabilizing the dimerized state (see Fig. 10). However, decreasing the lattice constant further, we found a point ($a$

$=1.3a_0$ for $Li_{10}$), below which the equidistant arrangement is the ground state, which would imply a metallic state for the infinite chain. At the HF level, a bond alternation is found for all (average) lattice constants; electronic correlations seem to suppress this bond alternation at the equilibrium lattice constant. This is in contrast to polyacetylene, where correlations reduce the bond alternation without fully suppressing it.[27]

## VIII. CONCLUSIONS

We investigated the analog of the metal-insulator transition for one-dimensional lithium, applying high-level quantum-chemical *ab initio* methods. The aim of this investigation was to find out how the MIT is modified from the one in the Hubbard model when we have to deal with several orbitals per site. We have chosen Li as an example since here the different orbitals correspond to different angular momentum quantum numbers, i.e., $s$ and $p$ electrons. By treating a $Li_{10}$ ring we could apply accurate quantum-chemical ab initio methods. Following the original ideas of Mott, a metallic system will become an insulator when the lattice constant is sufficiently large. But in distinction to the Hubbard model it is here the interplay of the $s$ and $p$ orbitals which strongly affects the MIT. At the transition point ($a_{MIT} \approx 1.5a_0$) the character of the many-body wave function changes from significant $p$ to essentially $s$ character. Therefore it must be kept in mind that in a real solid the repopulation of orbitals belonging to different angular momenta may have similarly strong influence on the MIT as changes in the ratio of the Hubbard $U$ to the kinetic energy. We found that approximately at the same interatomic distance where the $p$ character of the wave function changes so strongly, the one-particle energy gap is minimal and the static electric polarizability has a maximum. Increasing the ring length, the minimal gap closes faster than the gap at the equilibrium distance; the reduced level spacing for both longer rings and larger lattice constants enhances dynamical correlation effects. Allowing for a bond alternation in the ring, the system dimerizes for all (average) lattice constants larger than $\sim 1.3a_0$, for the insulating case due to $Li_2$ molecule formation, for the metallic case due to Peierls distortion. For even smaller lattice constants, the correlations stabilize the equidistant arrangement of the Li atoms along the ring.

Further investigations are planned for open boundary conditions (i.e., linear fragments of the infinite chain) and for other alkali metals (thereby, e.g., mixing different alkali-metal atoms to mimic the ionic Hubbard model).

## APPENDIX: LIST OF ABBREVIATIONS

| | |
|---|---|
| MIT | metal-insulator transition |
| HOMO | highest occupied molecular orbital |
| LUMO | lowest unoccupied molecular orbital |
| GTO | Gaussian-type orbital |
| cc-pVDZ | correlation-consistent polarized valence double-$\zeta$ |
| HF | Hartree-Fock |

| | | | |
|---|---|---|---|
| MCSCF | multiconfiguration self-consistent-field approximation | EA | electron affinity |
| MRCI | multireference configuration interaction | DFT | density-functional theory |
| MRACPF | multireference averaged coupled pair functional | LDA | local-density approximation |
| | | GGA | generalized gradient corrected approximation |
| IP | ionization potential | FCI | full CI—configuration interaction with all excitations |

*Present address: Institute of Physics, Jagellonian University, Reymonta 4, Pl 30-059 Krakow, Poland.

[1] N. F. Mott, *Metal-Insulator Transition*, 2nd ed. (Taylor and Francis, London, 1990).

[2] J. Hubbard, Proc. R. Soc. London, Ser. A **276**, 238 (1963); **277**, 237 (1963).

[3] F. Gebhard, *The Mott Metal-Insulator Transition* (Springer, Berlin, 1997).

[4] R.J. Gdanitz and R. Ahlrichs, Chem. Phys. Lett. **143**, 413 (1988).

[5] H.-J. Werner and P.J. Knowles, Theor. Chim. Acta **78**, 175 (1990).

[6] H.-J. Werner and P. J. Knowles with contributions from J. Almlöf, R. D. Amos, A. Bernhardsson, A. Berning, P. Celani, D. L. Cooper, M. J. O. Deegan, A. J. Dobbyn, F. Eckert, C. Hampel, G. Hetzer, T. Korona, R. Lindh, A. W. Lloyd, S. J. McNicholas, F. R. Manby, W. Meyer, M. E. Mura, A. Nicklass, P. Palmieri, R. Pitzer, G. Rauhut, M. Schütz, H. Stoll, A. J. Stone, R. Tarroni, and T. Thorsteinsson, computer code MOLPRO, version 2002.6 (University of Stuttgart, Stuttgart, Germany, 2002).

[7] P.J. Knowles and H.-J. Werner, Chem. Phys. Lett. **145**, 514 (1988).

[8] H.-J. Werner and P.J. Knowles, J. Chem. Phys. **89**, 5803 (1988).

[9] T.H. Dunning, Jr., J. Chem. Phys. **90**, 1007 (1989).

[10] C. Kittel, *Introduction to Solid State Physics*, 7th ed. (Wiley, New York, 1996).

[11] A.A. Radzig and B.M. Smirnov, *Reference Data on Atoms, Molecules, and Ions*, edited by J.P. Toennies, Springer Series in Chemical Physics, Vol. 31 (Springer, Berlin, 1985).

[12] V.R. Saunders, R. Dovesi, C. Roetti, M. Causa, N.M. Harrison, R. Orlando, and C.M. Zicovich-Wilson, *Crystal 98 User's Manual* (University of Torino, Torino, 1998).

[13] W.D. Knight, K. Clemenger, W.A. de Heer, and W.A. Saunders, Phys. Rev. B **31**, 2539 (1985).

[14] K. Doll, N.M. Harrison, and V.R. Saunders, J. Phys.: Condens. Matter **11**, 5007 (1999).

[15] R. Ahlrichs, M. Bäar, H.-P. Baron, R. Bauernschmitt, S. Böcker, M. Ehrig, K. Eichkorn, S. Elliott, F. Furche, F. Haase, M. Häser, H. Horn, C. Huber, U. Huniar, M. Kattannek, C. Kölmel, M. Kollwitz, K. May, C. Ochsenfeld, H. Öhm, A. Schäfer, U. Schneider, O. Treutler, M. von Armin, F. Weigend, P. Weis, and H. Weiss, computer code TURBOMOLE, version 5 (University of Karlsruhe, Karlsruhe, Germany, 2000). M. Häser, and R. Ahlrichs, J. Comput. Chem. **10**, 104 (1989); R. Ahlrichs, M. Bär, M. Häser, H. Horn, and C. Kölmel, Chem. Phys. Lett. **162**, 165 (1989).

[16] T.A. Koopmans, Physica **1**, 104 (1933).

[17] S.J. Vosko, L. Wilk, and M. Nusair, Can. J. Phys. **58**, 1200 (1980).

[18] A.D. Becke, Phys. Rev. A **38**, 3098 (1988).

[19] C. Lee, W. Yang, and R.G. Parr, Phys. Rev. B **37**, 785 (1988).

[20] H.-J. Werner and P.J. Knowles, J. Chem. Phys. **82**, 5053 (1985).

[21] P.J. Knowles and H.-J. Werner, Chem. Phys. Lett. **115**, 259 (1985).

[22] B. Paulus, Chem. Phys. Lett. **371**, 7 (2003).

[23] P.J. Knowles and N.C. Handy, Chem. Phys. Lett. **111**, 315 (1984).

[24] R. Antoine, D. Rayane, A.R. Allouche, M. Aubert-Frecon, E. Benichou, F.W. Dalby, Ph. Dugourd, M. Broyer, and C. Guet, J. Chem. Phys. **110**, 5568 (1999).

[25] E. Benichou, R. Antoine, D. Rayane, B. Vezin, F.W. Dalby, Ph. Dugourd, and M. Broyer, Phys. Rev. A **59**, R1 (1999).

[26] R. E. Peierls, *Quantum Theory of Solids* (Clarendon, London, 1955).

[27] G. König and G. Stollhoff, Phys. Rev. Lett. **65**, 1239 (1990).